NAVAL SHIP RESEARCH AND DEVELOPMENT CENTER
Washington, D. C. 20034

FIELD-POINT PRESSURES IN THE VICINITY OF A SERIES OF SKEWED MARINE PROPELLERS

by

Stephen S. Teel
and
Stephen B. Denny

DEPARTMENT OF HYDROMECHANICS
RESEARCH AND DEVELOPMENT REPORT

August 1970 Report 3278

DEPARTMENT OF THE NAVY
NAVAL SHIP RESEARCH AND DEVELOPMENT CENTER
WASHINGTON, D. C. 20034

FIELD-POINT PRESSURES IN THE VICINITY OF A SERIES OF SKEWED MARINE PROPELLERS

by

Stephen S. Teel
and
Stephen B. Denny

August 1970 Report 3278

TABLE OF CONTENTS

LIST OF FIGURES

LIST OF TABLES

NOTATION

A_E	Expanded blade area
A_0	Disk area, $\pi D^2/4$
A_E/A_0	Expanded area ratio
a_m	Fourier cosine coefficient of the m th harmonic of the pressure signal
a_0	Constant term, pressure signal
a_z	Fourier cosine coefficient of the blade-rate harmonic of the pressure signal
b_m	Fourier sine coefficient of the m th harmonic of the pressure signal
b_z	Fourier sine coefficient of the blade-rate harmonic of the pressure signal
C_{TA}	Thrust loading coefficient, $C_{TA} = \frac{8}{\pi J^2} K_T$
c	Blade section chord length
c_m	Amplitude of the m th harmonic of the pressure signal, $c_m = [a_m^2 + b_m^2]^{1/2}$
c_z	Amplitude of the blade-rate harmonic of the pressure signal
D	Propeller diameter
f_M	Blade section camber
J	Advance coefficient, $J = \frac{V_a}{ND}$
K_p	Nondimensional pressure coefficient, $K_p = \frac{p}{\rho N^2 D^2}$
K_{p_z}	Nondimensional blade-rate pressure coefficient, $K_{p_z} = \frac{(\Delta p)_z}{\rho N^2 D^2}$

K_T	Thrust coefficient
$\overline{K}_T$	Mean thrust coefficient
N	Propeller revolutions
P	Propeller blade section pitch
p	Pressure
$(\Delta p)_s$	Blade-rate pressure amplitude fluctuation
R	Propeller radius
$R_{n_{0.7}}$	Reynolds number at $0.7R$, $R_{n_{0.7}} = \dfrac{c_{0.7}\sqrt{V_A^2 + (0.7\pi ND)^2}}{\nu}$
r	Radial distance from propeller axis
T	Propeller thrust
t	Propeller blade section maximum thickness
V_a	Apparent propeller advance velocity
V_s	Ship velocity
x	Axial distance from propeller plane
Z	Blade number
s	Subscript depicting blade number or blade rate
β	Advance angle
β_i	Hydrodynamic pitch angle
γ	Dummy phase angle
θ	Phase angle of peak blade-rate pressure amplitude relative to reference line
θ_s	Blade skew angle relative to reference line
ν	Kinematic viscosity
ρ	Mass density of fluid
ϕ	Dummy phase angle

ABSTRACT

Total fluctuating pressures were measured on a flat plate adjacent to a model propeller operating in the 24-inch water tunnel. The effects of blade skew on propeller-induced field pressures are shown. The amplitude and phase of the blade-rate portions of the measured induced pressures are compared with the Kerwin prediction of propeller field-point pressures for operation in uniform flow at the design advance coefficient and for two propeller tip clearances. Experimental results and theoretical predictions for total field-point pressures were in good agreement for both amplitude and phase.

In addition to the measurements made in uniform flow, induced pressures were also measured for the propellers operating in nonuniform flows generated by 4- and 5-cycle wake screens placed upstream of the propeller. Experimental results of tests in uniform and nonuniform flow at the same mean thrust coefficient showed that increasing blade skew had the effect of reducing propeller-induced pressures and that increasing blade skew displaced the peak amplitude signal farther downstream.

ADMINISTRATIVE INFORMATION

This work was performed under the General Hydromechanics Research Program of the Naval Ship Research and Development Center (NSRDC). Funding was provided by NAVSHIPS Subproject S-R009-0101, Problem 526-356.

INTRODUCTION

The study of propeller-induced field pressures described here is part of an extensive investigation into the design and performance of skewed propellers. The model propeller series tested consists of four propellers with 0, 36, 72, and 108 degrees of blade skew; all were designed to perform identically at the same design advance condition. The propellers were designed using lifting-surface corrections derived by the Cheng procedure,[1] and pitch corrections due to thickness were calculated by the Kerwin method.[2] Open-water and cavitation performance,[3] and backing characteristics[4] of the four designs have been reported. In addition to these performance studies, an experimental program was undertaken to determine the stress levels which might be expected to exist in uniformly loaded, highly skewed propeller blades.[5] The effects of blade skew on unsteady propeller forces transmitted through the propeller shaft have been determined[6] in experiments using the skewed propeller series and employing six-component dynamometry and test procedures[7] developed earlier.

---

[1]References are listed on page 24.

This report will focus on the pressures transmitted by the propellers through the surrounding fluid. However, much of the experimental work was conducted concurrently with the fluctuating force measurements; the interrelation between oscillating field pressures and shaft forces are presented in Reference 6.

Propeller-induced pressure measurements as available from earlier studies by Tachmindji,[8] Kowalski,[9] Denny,[10] and others; however, only limited information is given on the effects of skew and there is no systematic analysis of skew. Therefore, it was the purpose of this study to determine experimentally the effects of blade skew on induced field pressures and to compare the findings with theoretical predictions if possible.

The test procedure selected was essentially the same as that used by Denny in 1967.[10] Pressures were measured on a flat plate positioned parallel to the propeller rotation axis, and the transducers were located axially from upstream to downstream of the propeller plane such that normals to the plate at each transducer would intersect the propeller axis.

Experimentally determined pressures were compared with theoretical predictions of the Kerwin procedure.[11] The Kerwin method is an extension of his lifting-surface propeller design theory[12] and is applicable to moderately loaded propellers. It is based on a vortex lattice representation of blade loading and utilizes a linearized source-sink distribution to represent blade thickness. A pointwise distribution of the axial, radial, and tangential velocities is calculated relative to a propeller blade, a harmonic analysis is performed, and the linearized, blade-rate pressure coefficient is derived from the induced velocities.

Since the predictions are for free-space propeller-induced pressures, all predicted pressure amplitudes were doubled for comparison with the experimental results under the assumption of a pure image effect, thus satisfying the boundary condition at the flat plate. Although experimental results were obtained and are presented for the propeller operating in uniform and nonuniform flows and at a variety of advance conditions, comparisons with theoretical predictions were restricted to the case of uniform inflow at design advance coefficients. The restriction of uniform flow was imposed since the Kerwin theory for field-point pressure calculation precludes any circumferentially varying inflow. Only the design advance cases were compared. Although it is possible to alter the magnitude of propeller loading input into the Kerwin procedure and to adjust the hydrodynamic pitch distribution input, no reliable procedure has been published for estimating the radial distribution of loading or hydrodynamic pitch for a given propeller at an off-design advance condition.

TEST PROCEDURE

Tests were run in the closed-jet test section of the 24-inch water tunnel with the propellers fitted on the downstream shaft. A flat plate was mounted parallel to the propeller axis and contained five transducers located on a line nearest to and parallel to the propeller axis. The flat plate dimensions, transducer locations, and placement in the water tunnel are shown in Figure 1. A plane through the hub midlength and perpendicular to the shaft axis

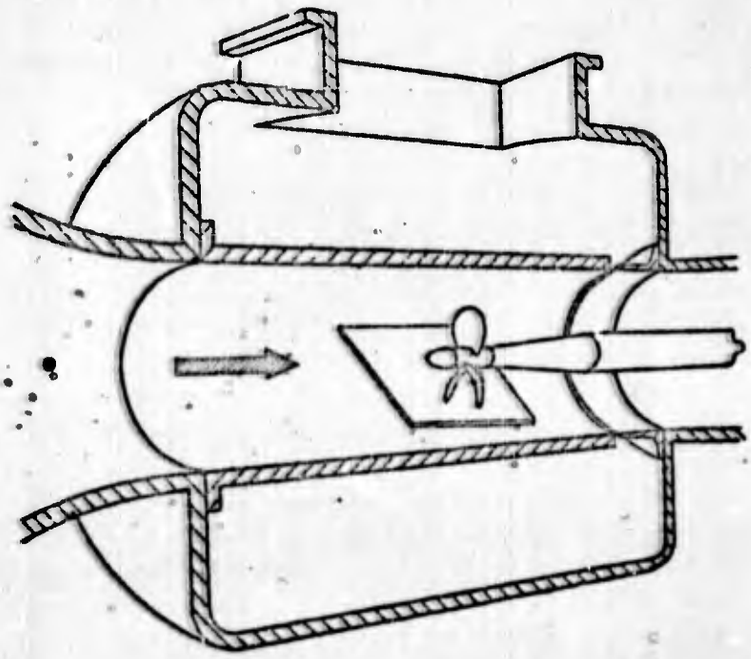

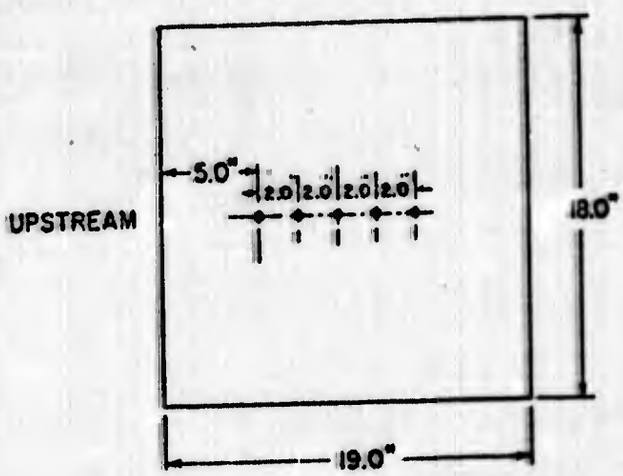

Figure 1 – Flat Plate Dimensions and Placement in the Water Tunnel

was used as a reference plane for the presentation of data. This plane intersected the flat plate near the center transducer. The plate was positioned at two propeller tip clearances, 10 and 30 percent of the propeller radius. Because skewed propellers have a natural rake, the blade tips of the 0-, 36-, 72-, and 108-degree skewed propellers were respectively located at approximately 0, 25, 41.7, and 58.3 percent of the propeller radius downstream of the reference plane.

The presence of the flat plate made it necessary to assume a pure image system and, consequently, to double the free-space calculated pressures for comparison with the experimental results. However, since the pressures are calculated from the induced field-point axial and tangential velocities, it was also necessary that normals to the transducers intersect the propeller axis, thus ensuring that the tangential induced velocities are, in fact, the transverse velocities at the transducers. Should this not be the case, a complicated pointwise resolution of the induced tangential and radial velocities would be necessary to determine the transverse induced velocity in the plane of the plate and at each transducer.

The propellers tested were 12 inches in diameter, and contained five blades. They had 0, 36, 72, and 108 degrees of skew and were designated as Models 4381, 4382, 4383, and 4384, respectively. All four were designed to perform identically at the same design advance coefficient. The only geometrical differences in the propellers were their degree of skew and the radial pitch and camber corrections due to skew. Table 1 gives pertinent geometry for the propeller series and Figure 2 is a photograph of the propellers.

Advance coefficients for the tests were determined by setting a thrust identity with the open-water test results. Nonuniform flow was generated for some of the tests by the use of wake screens,[13] and the advance coefficients were then based on a mean thrust coefficient. Thrust coefficients established during the tests of all propellers were $K_T = 0.0$, 0.100, 0.215, 0.300, 0.375, and 0.400. Table 2 indicates the $K_T - J$ relations in open water for the four propellers. Shaft revolutions were maintained at 14.0 rps for all testing.

In nonuniform flow tests with the 4- and 5-cycle wake screens, the effect of each distinct flow region on induced pressures was investigated. Figures 3 and 4 are diagrams of the wake screens. The position designated on the diagrams are those points positioned directly upstream of and in line with the five measuring transducers.

TABLE 1

Geometry of Propellers

Number of Blades	5
Expanded Area Ratio, A_E/A_0	0.725
Section Meanline	NACA $a = 0.8$
Section Thickness Distribution	NACA 66 with NSRDC modified nose and tail
Design K_T	0.215
Design C_P	0.534

r/R	$\tan \beta_i$	c/D	t_0/c
0.2	1.8256	0.174	0.2694
0.3	1.3094	0.229	0.1562
0.4	1.0075	0.275	0.1068
0.5	0.8034	0.312	0.0768
0.6	0.6483	0.337	0.0566
0.7	0.5300	0.342	0.0421
0.8	0.4390	0.334	0.0314
0.9	0.3651	0.299	0.0239

Propeller 4381 (Skew - 0 Degrees)

r/R	θ_s (degrees)	P/D	l_M/c
0.3	0.0	1.3448	0.0360
0.4	0.0	1.3580	0.0348
0.5	0.0	1.3361	0.0307
0.6	0.0	1.2797	0.0245
0.7	0.0	1.2059	0.0191
0.8	0.0	1.1366	0.0148
0.9	0.0	1.0660	0.0123

Propeller 4382 (Skew - 36 Degrees)

r/R	θ_s (degrees)	P/D	l_M/c
0.3	4.655	1.4332	0.0370
0.4	9.383	1.4117	0.0344
0.5	13.948	1.3613	0.0305
0.6	18.378	1.2858	0.0247
0.7	22.747	1.1999	0.0199
0.8	27.145	1.1117	0.0161
0.9	31.595	1.0270	0.0134

Propeller 4383 (Skew - 72 Degrees)

r/R	θ_s (degrees)	P/D	l_M/c
0.3	9.293	1.5124	0.0407
0.4	18.816	1.4268	0.0365
0.5	27.991	1.3260	0.0342
0.6	36.770	1.2138	0.0281
0.7	45.453	1.1976	0.0230
0.8	54.245	1.0939	0.0189
0.9	63.102	0.9955	0.0159

Propeller 4384 (Skew - 108 Degrees)

r/R	θ_s (degrees)	P/D	l_M/c
0.3	13.921	1.5832	0.0479
0.4	28.426	1.4956	0.0453
0.5	42.152	1.4057	0.0401
0.6	55.199	1.3051	0.0334
0.7	68.098	1.1993	0.0278
0.8	81.283	1.0864	0.0232
0.9	94.624	0.9729	0.0193

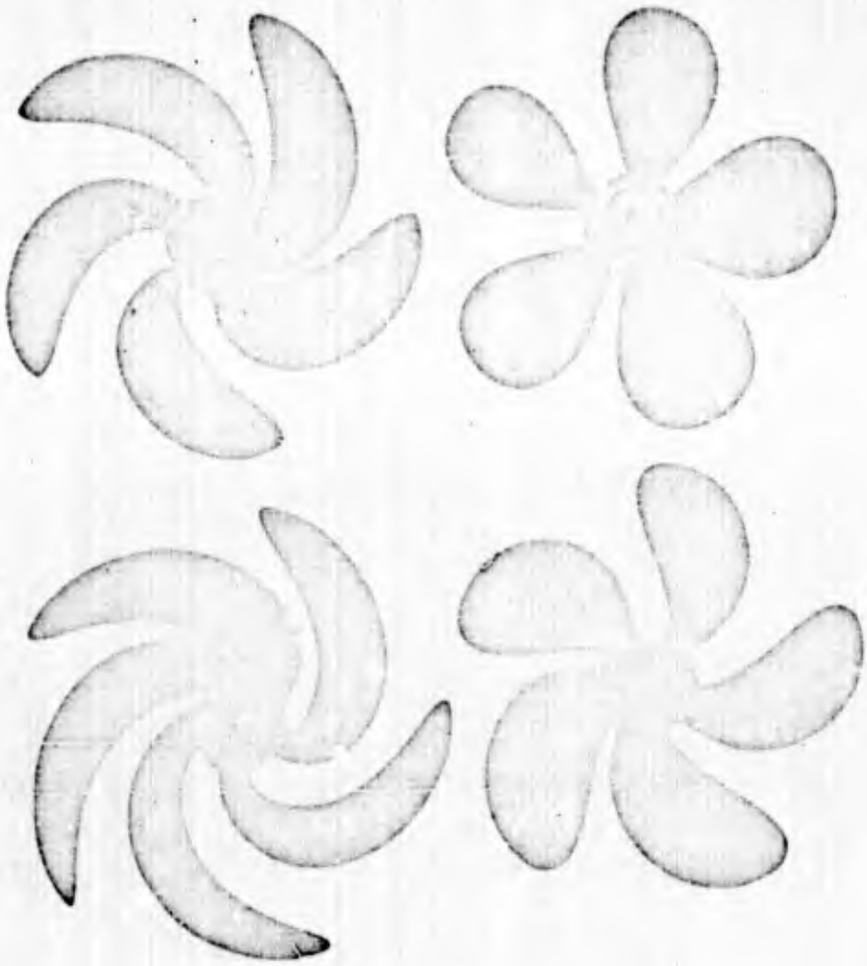

Figure 2 – Skewed Propeller Series

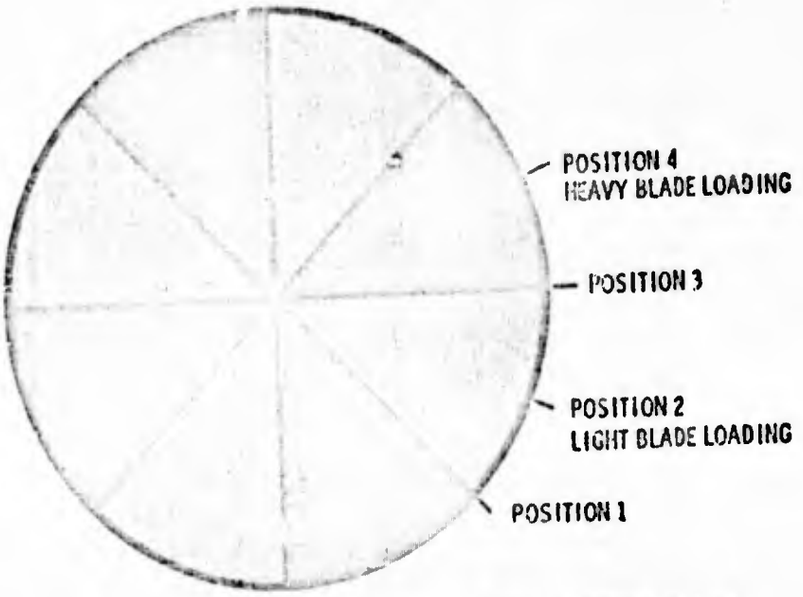

Figure 3 – 4-Cycle Wake Screen Showing Distinct Regions of Flow

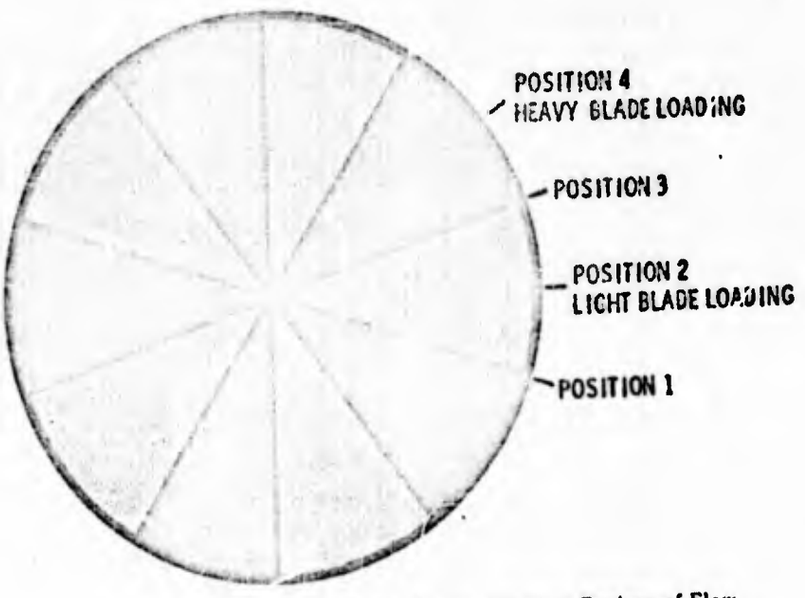

Figure 4 – 5-Cycle Wake Screen Showing Distinct Regions of Flow

TABLE 2

Open-Water Advance Coefficients at the Thrust Coefficients Selected for Tunnel Tests

(K_T = 0.000, 0.100, 0.215, 0.300, 0.375, and 0.400.)

Propeller Number	Skew degrees	Advance Coefficients					
4381	0	1.280	1.118	0.873	0.688	0.538	0.493
4382	36	1.290	1.108	0.865	0.680	0.535	0.485
4383	72	1.293	1.143	0.887	0.695	0.527	0.478
4384	108	1.297	1.127	0.873	0.659	0.476	0.417

DATA ANALYSIS

Pressure measured at each transducer was recorded on magnetic tape. The records of at least 100 propeller revolutions at each test condition were digitized and averaged, and the average wave form data were then entered into a computerized harmonic analysis routine. In general, the blade-rate harmonic was the most significant for all the test results. At high advance coefficient–low blade loading conditions, however, the shaft harmonic tended to be a sizeable portion of the total pressure signal. This can be attributed to slight shaft misalignment or even manufacturing differences in the blades.

The unsteady pressure measured at each transducer can be represented by a Fourier series as:

$$p = \frac{a_0}{2} + \sum_{m=1}^{\infty} a_m \cos m\phi + b_m \sin m\phi \qquad (1)$$

and the blade-rate pressure amplitude would be:

$$(\Delta p)_z = c_z = [(a_z)^2 + (b_z)^2]^{1/2} \qquad (2)$$

where z is the number of blades.

The phase of the blade-rate signal was derived from:

$$p = \frac{a_0}{2} + \sum_{m=1}^{\infty} c_m \left(\frac{a_m}{c_m} \cos m\phi + \frac{b_m}{c_m} \sin m\phi \right)$$

by letting

$$\frac{a_m}{c_m} = \cos\gamma \quad \text{and} \quad \frac{b_m}{c_m} = \sin\gamma$$

Therefore

$$p = \frac{a_0}{2} + \sum_{m=1}^{\infty} c_m \cos(m\phi - \gamma)$$

and by neglecting all terms except those of blade rate

$$\tan\gamma = \frac{b_z}{a_z} \quad \text{or} \quad \gamma = \tan^{-1}\left(\frac{b_z}{a_z}\right)$$

The maximum blade-rate signal occurs when $(z\phi - \gamma) = 0$. Therefore when $\phi = \gamma/z$, the phase angle θ for which $(\Delta p)_z$ is a maximum is defined to be

$$\theta = \frac{1}{z}\tan^{-1}\frac{b_z}{a_z} \tag{3}$$

The experimental pressure amplitudes were then nondimensionalized as follows:

$$K_{P_z} = \frac{(\Delta p)_z}{\rho N^2 D^2}$$

DISCUSSION OF RESULTS

UNIFORM FLOW – DESIGN ADVANCE COEFFICIENT

Total blade-rate-induced pressure amplitudes and phases measured on a flat plate with the propellers operating at design advance coefficient were compared with theoretical predictions. The predictions of Kerwin theory were derived from calculated induced velocities due to the bound vortices on the blades, the free vortices shed from the lifting lines (corrected on the blade), and the thickness effects. These induced velocities were then added in phase and a linearized blade-rate pressure coefficient computed from the harmonic analysis of the resultant velocity distribution.

Figures 5–8 and Figures 9–12 compare experimental results and theoretical predictions for propeller tip clearances of 10- and 30-percent radius, respectively.

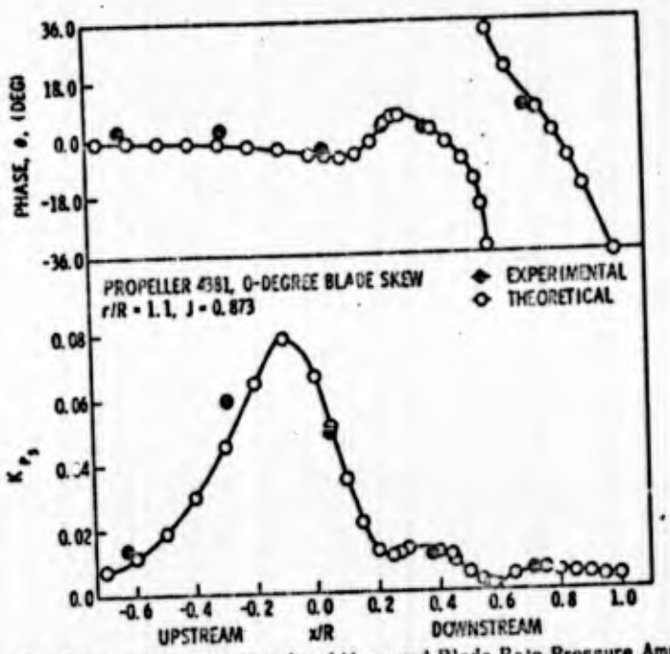

Figure 5 – Comparison of Predicted and Measured Blade-Rate Pressure Amplitudes and Phases for Design Advance Coefficient $J = 0.873$, 0-Degree Blade Skew, and 10-Percent Propeller Radius Tip Clearance

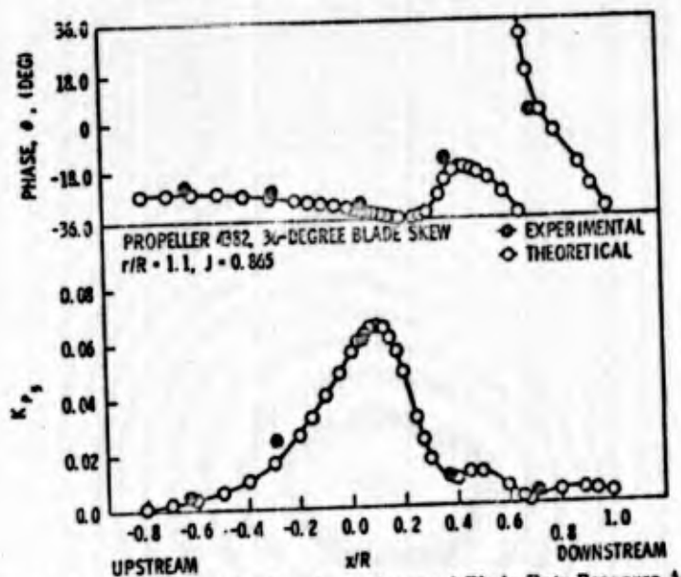

Figure 6 – Comparison of Predicted and Measured Blade-Rate Pressure Amplitudes and Phases for Design Advance Coefficient $J = 0.865$, 36-Degree Blade Skew, and 10-Percent Propeller Radius Tip Clearance

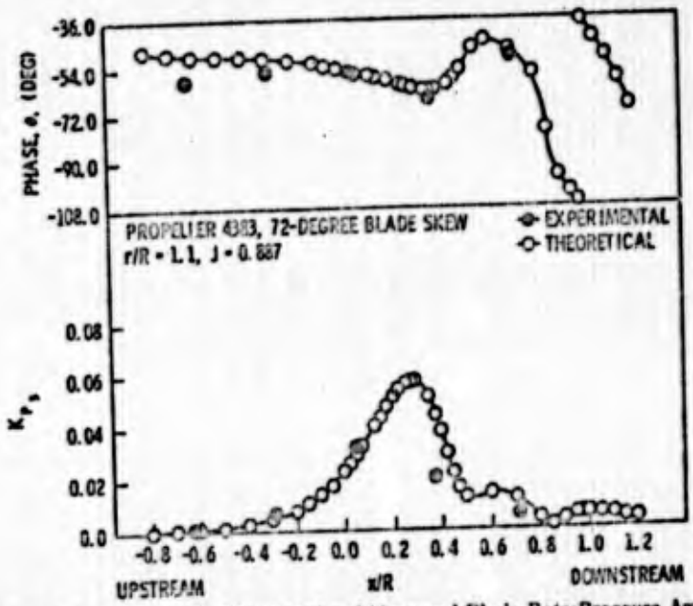

Figure 7 – Comparison of Predicted and Measured Blade-Rate Pressure Amplitudes and Phases for Design Advance Coefficient $J = 0.887$, 72-Degree Blade Skew, and 10-Percent Propeller Radius Tip Clearance

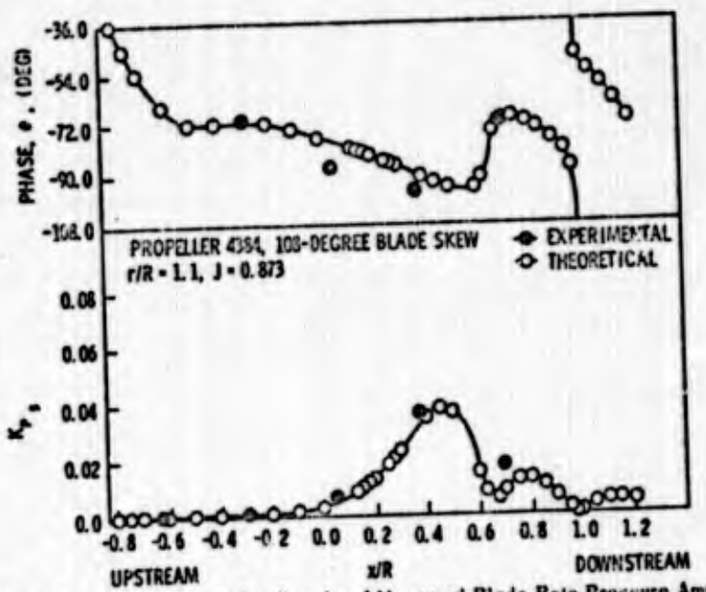

Figure 8 – Comparison of Predicted and Measured Blade-Rate Pressure Amplitudes and Phases for Design Advance Coefficient $J = 0.873$, 108-Degree Blade Skew, and 10-Percent Propeller Radius Tip Clearance

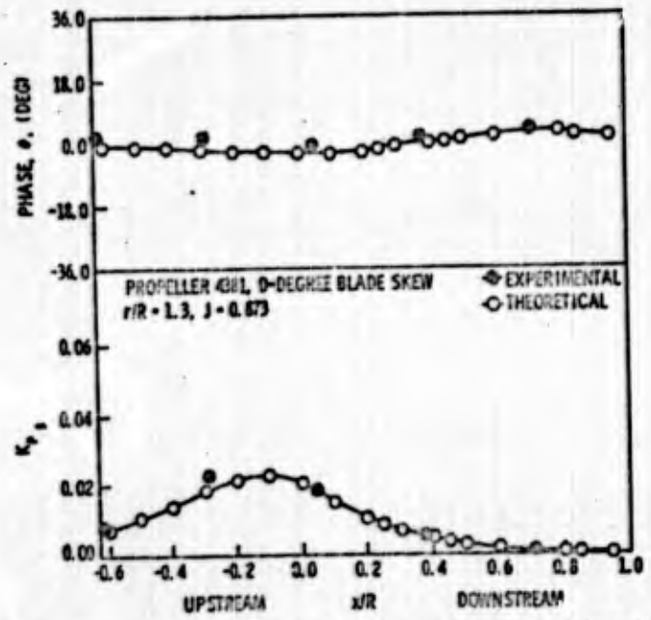

Figure 9 – Comparison of Predicted and Measured Blade-Rate Pressure Amplitudes and Phases for Design Advance Coefficient $J = 0.873$, 0-Degree Blade Skew, and 30-Percent Propeller Radius Tip Clearance

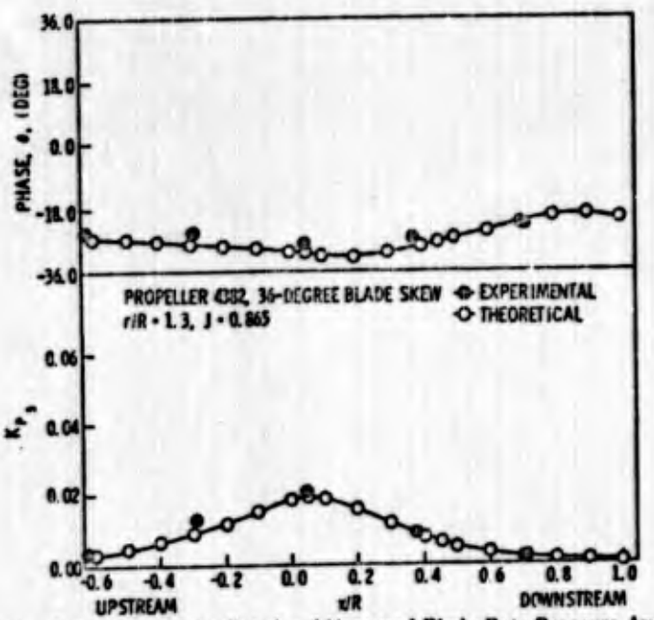

Figure 10 – Comparison of Predicted and Measured Blade-Rate Pressure Amplitudes and Phases for Design Advance Coefficient $J = 0.865$, 36-Degree Blade Skew, and 30-Percent Propeller Radius Tip Clearance

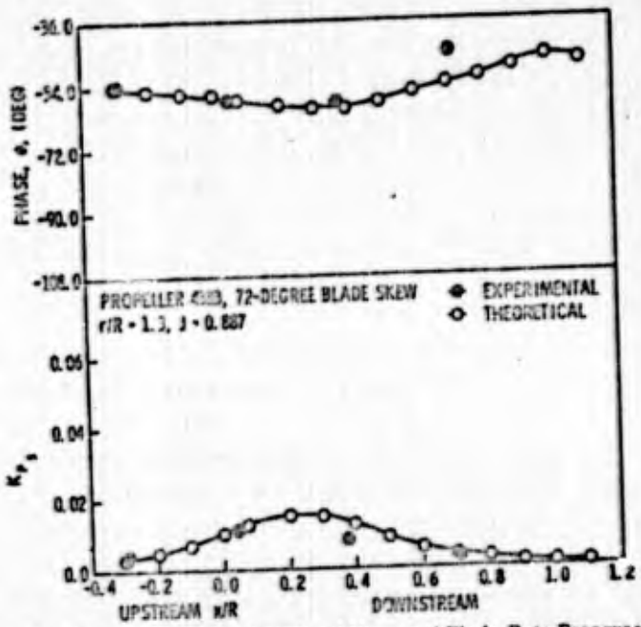

Figure 11 – Comparison of Predicted and Measured Blade-Rate Pressure Amplitudes and Phases for Design Advance Coefficient $J = 0.887$, 72-Degree Blade Skew, and 30-Percent Propeller Radius Tip Clearance

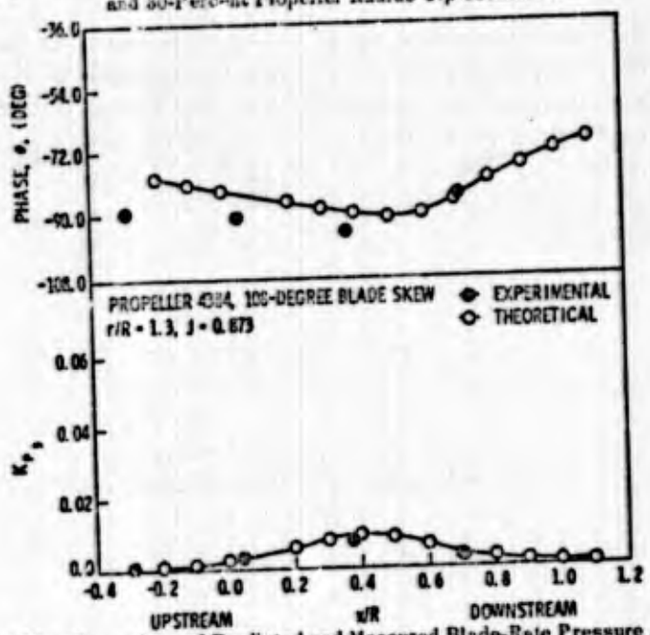

Figure 12 – Comparison of Predicted and Measured Blade-Rate Pressure Amplitudes and Phases for Design Advance Coefficient $J = 0.873$, 108-Degree Blade Skew, and 30-Percent Propeller Radius Tip Clearance

The pressure amplitudes are presented in the form of nondimensionalized blade-rate coefficients with the predicted values being twice the free-space calculations. The plots show amplitude and phase versus axial distance from the propeller plane with the $x/R = 0$ position designating the propeller reference plane. Phase is defined as the angular difference between the circumferential location of the maximum blade-rate pressure signal and a reference line extending from the hub center through the blade hub section midchord and lying in the propeller reference plane.

A comparison of Figures 5–8 and Figures 9–12 indicates the large decrease of blade-rate pressure amplitude with increased clearance from the propeller blade tips. The increase in clearance from 10 to 30 percent of the propeller radius reduced the maximum pressures 70 to 75 percent for the four propellers. The curves of predicted pressure coefficients at the 10-percent radius clearance show that the maximum pressure was reduced by 15, 27, and 61 percent for 36, 72, and 108 degrees of skew, respectively, over the value for the nonskewed propeller. Also, the maximum pressure signal was displaced farther downstream with increasing skew at both clearances. The maximum pressures were located at 10 percent of the radius upstream of the nonskewed propeller plane and about 8, 25, and 44 percent of the radius downstream of the propeller plane for the 36-, 72-, and 108-degree skewed propellers, respectively. These comparisons were made for the propellers operating in uniform flow and at the design advance coefficient.

The agreement between experimental and predicted values appears to be better than that found by Denny[10] even though the skewed propeller series exhibits far more complicated geometries. This may be due to several factors. The individual blades of the five-bladed skewed propellers were more lightly loaded (a reduction of approximately 20 percent in loading) than the three-bladed propellers tested in the previous work, and the lighter loading could lead to better agreement with the mathematical model. A second factor could be the possibility that the divergent downstream propeller shaft used in the skewed propeller tests may have affected both propeller performance and slipstream deformation to some extent. The program used for the pressure predictions shown here was an updated version; however, a check between the predictions and those of the original program for an identical input case showed that the differences were small and not accountable for the improved agreement.

Tables 3–6 give detailed information on the predicted blade-rate amplitudes and phases shown in Figures 5–12. It should be noted that the ordinate scale of the phase plots depicts the angular lead (or lag) from the blade reference line. Downstream of the propeller plane, it can be seen that the predicted phase curve may sweep the ordinate range of the plot. This sweep can be interpreted either as an additional 72 degrees of lag in the maximum blade-rate amplitude signal or as the appearance of the lagging signal of the previous blade.

It can be seen that phase lag is a function of both the degree of blade skew and distance of the field point from the propeller plane. The definition of the blade reference line location accounts for the appearance in the plots of phase lag due to skew and evident at the propeller reference plane.

TABLE 3

Predicted Blade-Rate Pressure Amplitude and Phase for Propeller 4381

(0-Degree Skew)

r/R = 1.10			r/R = 1.30	
z/R	K_{P_z}	Phase	K_{P_z}	Phase
-0.700	0.0068	- 0.5	0.0046	-1.0
-0.600	0.0112	- 0.6	0.0070	-1.3
-0.500	0.0164	- 0.8	0.0102	-1.6
-0.400	0.0226	- 1.1	0.0140	-1.9
-0.300	0.0454	- 1.5	0.0182	-2.2
-0.200	0.0646	- 2.2	0.0218	-2.7
-0.100	0.0782	- 3.2	0.0228	-3.2
0.000	0.0806	- 4.8	0.0204	-3.7
0.050	0.0510	- 5.6	0.0182	-3.8
0.100	0.0346	- 6.0	0.0156	-3.7
0.150	0.0212	- 5.2	0.0130	-3.4
0.200	0.0126	- 1.5	0.0106	-2.9
0.240	0.0108	3.5	0.0092	-2.4
0.250	0.0110	4.5	0.0088	-2.2
0.275	0.0116	6.1	0.0080	-1.9
0.300	0.0128	6.5	0.0072	-1.5

r/R = 1.10			r/R = 1.30	
z/R	K_{P_z}	Phase	K_{P_z}	Phase
0.400	0.0120	2.4	0.0050	-0.5
0.450	0.0090	- 1.4	0.0040	-0.1
0.500	0.0054	- 6.4	0.0032	0.2
0.540	0.0024	- 13.1	0.0026	0.6
0.560	0.0014	- 20.9	0.0024	0.9
0.580	0.0014	- 34.0	0.0022	1.2
0.600	0.0018	- 38.7	0.0022	1.4
0.620	0.0022	- 41.9	0.0020	1.5
0.650	0.0044	- 50.6	0.0018	2.4
0.750	0.0042	- 63.5	0.0006	2.8
0.800	0.0056	- 70.5	0.0010	2.3
0.850	0.0048	- 78.5	0.0008	1.5
0.900	0.0042	- 87.7	0.0006	0.9
0.950	0.0038	- 97.8	0.0004	1.2
1.000	0.0038	-107.9	0.0004	3.2

TABLE 4

Predicted Blade-Rate Pressure Amplitude and Phase for Propeller 4382

(36-Degree Skew)

r/R = 1.10			r/R = 1.30	
z/R	K_{P_z}	Phase	K_{P_z}	Phase
-0.800	0.0014	- 25.7	0.0012	-27.4
-0.700	0.0022	- 25.7	0.0018	-27.6
-0.600	0.0036	- 25.6	0.0026	-27.3
-0.500	0.0062	- 25.8	0.0042	-27.6
-0.400	0.0102	- 26.4	0.0062	-27.6
-0.300	0.0168	- 27.2	0.0086	-28.9
-0.200	0.0266	- 28.1	0.0120	-29.6
-0.150	0.0330	- 26.7	0.0128	-29.9
-0.100	0.0406	- 29.4	0.0154	-30.3
-0.050	0.0488	- 30.1	0.0170	-30.8
0.000	0.0570	- 31.0	0.0182	-31.2
0.025	0.0606	- 31.4	0.0184	-31.4
0.050	0.0626	- 31.9	0.0186	-31.6
0.075	0.0656	- 32.3	0.0186	-31.8
0.100	0.0662	- 32.8	0.0184	-32.0
0.125	0.0650	- 33.3	0.0178	-32.1
0.150	0.0616	- 33.7	0.0172	-32.2
0.175	0.0564	- 34.1	0.0164	-32.2
0.200	0.0492	- 34.4	0.0154	-32.2
0.225	0.0410	- 34.5	0.0140	-32.1
0.250	0.0324	- 34.4	0.0132	-32.0

r/R = 1.10			r/R = 1.30	
z/R	K_{P_z}	Phase	K_{P_z}	Phase
0.275	0.0244	- 34.8	0.0120	-31.8
0.300	0.0174	- 32.9	0.0108	-31.5
0.350	0.0090	- 26.3	0.0086	-30.6
0.375	0.0086	- 21.2	0.0078	-30.1
0.400	0.0098	- 18.1	0.0070	-29.5
0.425	0.0112	- 16.9	0.0062	-28.9
0.450	0.0122	- 17.0	0.0056	-28.2
0.475	0.0126	- 17.7	0.0050	-27.6
0.500	0.0124	- 18.8	0.0046	-27.1
0.540	0.0110	- 21.2	0.0040	-26.3
0.600	0.0070	- 26.0	0.0030	-25.9
0.650	0.0034	- 32.2	0.0024	-24.5
0.660	0.0026	- 34.2	0.0022	-24.3
0.680	0.0014	- 41.1	0.0020	-23.9
0.700	0.0012	- 54.9	0.0018	-23.5
0.750	0.0034	- 69.5	0.0016	-22.2
0.800	0.0050	- 76.2	0.0012	-21.0
0.900	0.0056	- 89.7	0.0010	-20.5
0.950	0.0050	- 96.7	0.0008	-21.2
1.000	0.0042	-105.5	0.0006	-22.8

TABLE 5

Predicted Blade Rate Pressure Amplitude and Phase for Propeller 4383

(72-Degree Skew)

r/R = 1.10			r/R = 1.30	
z/R	K_{P_z}	Phase	K_{P_z}	Phase
-0.800	0.0002	- 47.2	0.0004	-48.9
-0.700	0.0006	- 49.5	0.0006	-52.4
-0.600	0.0008	- 50.3	0.0008	-54.0
-0.500	0.0014	- 50.3	0.0012	-54.0
-0.400	0.0024	- 50.4	0.0020	-53.8
-0.300	0.0044	- 51.3	0.0032	-54.7
-0.200	0.0078	- 52.5	0.0048	-55.8
-0.150	0.0102	- 53.2	0.0058	-56.3
-0.100	0.0134	- 53.9	0.0070	-56.7
-0.050	0.0174	- 54.7	0.0084	-57.2
0.000	0.0226	- 55.6	0.0100	-57.7
0.025	0.0256	- 56.1	0.0108	-58.0
0.050	0.0288	- 56.6	0.0116	-58.3
0.075	0.0322	- 57.1	0.0124	-58.6
0.125	0.0396	- 58.3	0.0138	-59.2
0.150	0.0434	- 58.7	0.0144	-59.5
0.175	0.0472	- 59.5	0.0150	-59.8
0.200	0.0506	- 60.2	0.0154	-60.1
0.225	0.0536	- 60.8	0.0156	-60.4
0.250	0.0560	- 61.5	0.0156	-60.6
0.275	0.0570	- 62.1	0.0154	-60.8

r/R = 1.10			r/R = 1.30	
z/R	K_{P_z}	Phase	K_{P_z}	Phase
0.300	0.0566	- 62.7	0.0152	-60.9
0.350	0.0500	- 63.6	0.0140	-61.0
0.375	0.0438	- 63.7	0.0132	-60.9
0.400	0.0364	- 63.6	0.0124	-60.8
0.425	0.0288	- 63.1	0.0114	-60.5
0.450	0.0216	- 62.0	0.0104	-60.2
0.475	0.0156	- 59.8	0.0096	-59.8
0.500	0.0118	- 56.1	0.0086	-59.3
0.550	0.0112	- 47.9	0.0070	-58.0
0.600	0.0134	- 45.7	0.0058	-56.6
0.700	0.0114	- 49.2	0.0038	-54.1
0.800	0.0078	- 57.9	0.0026	-52.3
0.850	0.0068	- 79.5	0.0020	-51.2
0.900	0.0052	- 97.4	0.0016	-49.9
0.950	0.0050	-103.6	0.0014	-48.6
0.980	0.0054	-107.2	0.0012	-48.0
1.000	0.0056	-109.9	0.0012	-47.8
1.050	0.0054	-116.3	0.0010	-47.8
1.100	0.0048	-123.7	0.0008	-48.3
1.150	0.0040	-132.5	0.0006	-49.1
1.200	0.0036	-142.5	0.0004	-49.4

TABLE 6

Predicted Blade Rate Pressure Amplitude and Phase for Propeller 4384

(108-Degree Skew)

r/R = 1.10			r/R = 1.30	
z/R	K_{P_z}	Phase	K_{P_z}	Phase
-0.800	0.0000	- 36.0	0.0000	-29.3
-0.750	0.0000	- 44.3	0.0000	-40.7
-0.700	0.0000	- 54.0	0.0000	-54.0
-0.600	0.0000	- 65.4	0.0002	-72.0
-0.500	0.0002	- 72.0	0.0002	-79.7
-0.400	0.0002	- 72.0	0.0002	-81.0
-0.200	0.0010	- 71.4	0.0010	-79.5
-0.100	0.0020	- 74.1	0.0016	-81.6
0.000	0.0038	- 76.7	0.0024	-83.2
0.125	0.0068	- 80.3	0.0032	-84.0
0.150	0.0102	- 81.1	0.0048	-85.4
0.175	0.0120	- 82.0	0.0054	-85.9
0.200	0.0138	- 82.8	0.0060	-86.3
0.250	0.0184	- 84.7	0.0070	-87.3
0.275	0.0210	- 85.6	0.0076	-89.9
0.300	0.0238	- 86.6	0.0080	-88.3
0.400	0.0350	- 90 5	0.0094	-89.9

r/R = 1.10			r/R = 1.30	
z/R	K_{P_z}	Phase	K_{P_z}	Phase
0.450	0.0382	- 92.4	0.0094	-90.5
0.500	0.0366	- 94.1	0.0088	-90.8
0.600	0.0156	- 94.4	0.0064	-90.0
0.670	0.0082	- 91.1	0.0056	-89.2
0.675	0.0062	- 74.3	0.0044	-87.1
0.700	0.0090	- 70.6	0.0038	-86.1
0.750	0.0130	- 69.7	0.0032	-83.2
0.800	0.0132	- 71.2	0.0028	-80.1
0.850	0.0106	- 73.7	0.0024	-78.2
0.900	0.0066	- 77.0	0.0020	-76.4
0.950	0.0024	- 81.2	0.0018	-74.8
0.975	0.0004	- 87.3	0.0016	-73.9
1.000	0.0014	-119.4	0.0014	-73.0
1.050	0.0040	-124.8	0.0012	-71.3
1.100	0.0056	-130.0	0.0012	-70.0
1.150	0.0058	-135.7	0.0010	-69.5
1.200	0.0054	-142.4	0.0008	-69.8

UNIFORM FLOW – RANGE OF ADVANCE COEFFICIENTS

Figures 13 and 14 show the blade-rate pressure amplitudes measured with 36-degree Propeller 4382 operating at advance coefficients of 0.375, 0.3, 0.215, 0.100, and 0.0 at 10- and 30-percent propeller radius tip clearances, respectively. The limited test results have been connected by curves for visual clarity; the curves are not intended to depict trends in the axial pressure distribution. Figures 15 and 16 show the measured blade-rate pressure amplitudes for all four propellers of the series at 10-percent propeller radius tip clearance and at thrust coefficient values of $K_T = 0.375, 0.215, 0.100$, and 0.00.

The induced pressures observed in the various uniform flows exhibited similar trends in that the induced field pressures were greater at low advance-coefficient, high-loading conditions and the induced pressures were lessened at high advance-coefficient, lightly loaded conditions. The effect of skew was similar in that increasing skew reduced the induced pressures in comparable amounts regardless of the advance condition.

NONUNIFORM FLOW

Figure 17 compares the results of induced pressure measurements on a flat plate for Propellers 4381 (10-degree skew) and 4383 (72-degree skew) run at design advance conditions (mean thrust coefficient $\overline{K}_T = 0.215$) for each distinct position of the 4-cycle wake screen and at 10-percent propeller radius tip clearance. Position 4 produced the largest values of blade-rate induced pressures followed in magnitude by values obtained at Positions 3, 1, and 2, in that order. Position 4 corresponded to the region of heaviest propeller blade loading since the inflow velocity was least through that region of the screen. In contrast, Position 2 was the region of highest inflow velocity and the propeller blade loading was least in that region. The other positions were combinations of the high and low inflow regions, and values of blade-rate induced pressures were between those obtained at Positions 4 and 2. The nonuniform flow results showed reductions in blade-rate pressure signal with increasing skew comparable to those observed in the uniform flow results.

The results obtained for the various distinct regions of flow created by the 5-cycle wake screen showed similar trends to those obtained for the 4-cycle wake screen. Figures 18 and 19 present the values of blade-rate pressure measured on the flat plate for Propellers 4381 and 4383 operating in nonuniform flow created by the 4- and 5-cycle wake screens at 10-percent propeller radius tip clearance and at several advance conditions. Results are given for measurements obtained while the 5-cycle wake was in Position 3 and the 4-cycle wake was in Position 4. Problems with the data recorder occurred during tests with the 5-cycle wake at Position 4, and the data were not complete enough for presentation.

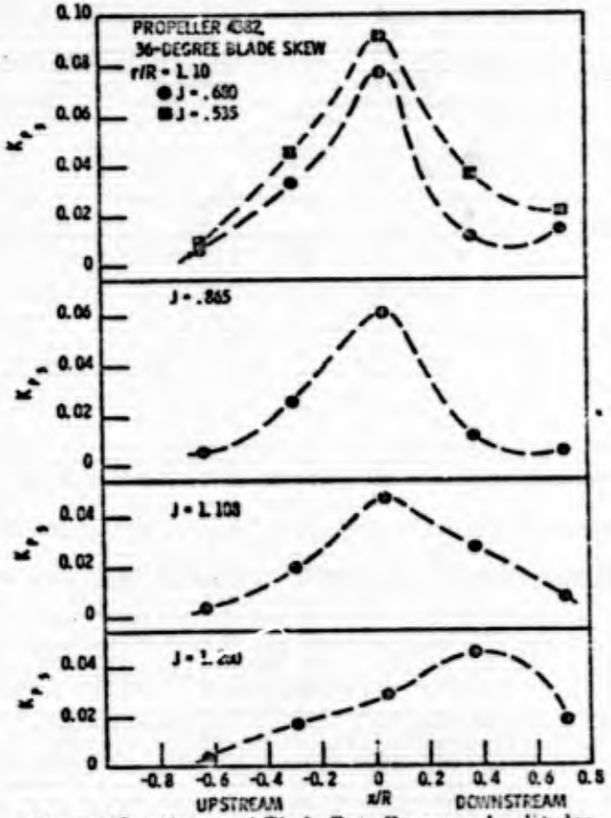

Figure 13 – Measured Blade-Rate Pressure Amplitudes for the 36-Degree Skewed Propeller at Five Advance Conditions and 10-Percent Propeller Radius Tip Clearance

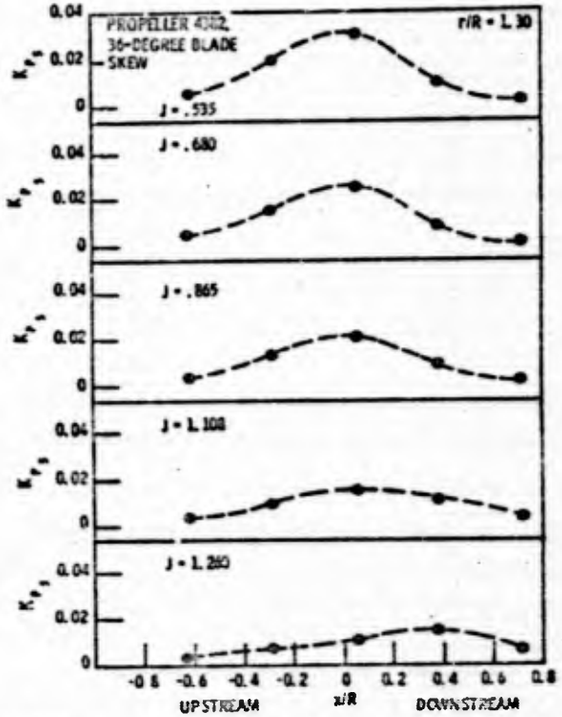

Figure 14 – Measured Blade-Rate Pressure Amplitudes for the 36-Degree Skewed Propeller at Five Advance Conditions and 30-Percent Propeller Radius Tip Clearance

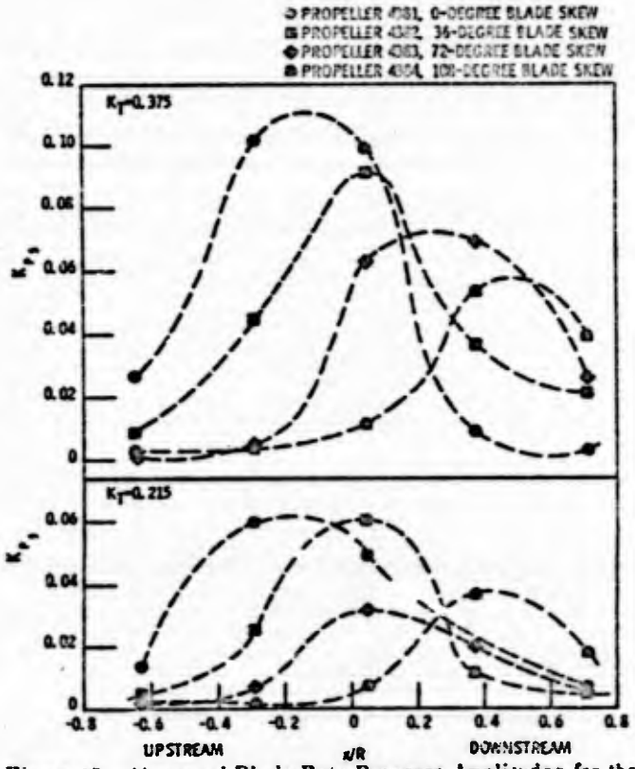

Figure 15 – Measured Blade-Rate Pressure Amplitudes for the Skewed Propeller Series at K_T = 0.375 and Design K_T = 0.215 for 10-Percent Propeller Radius Tip Clearance

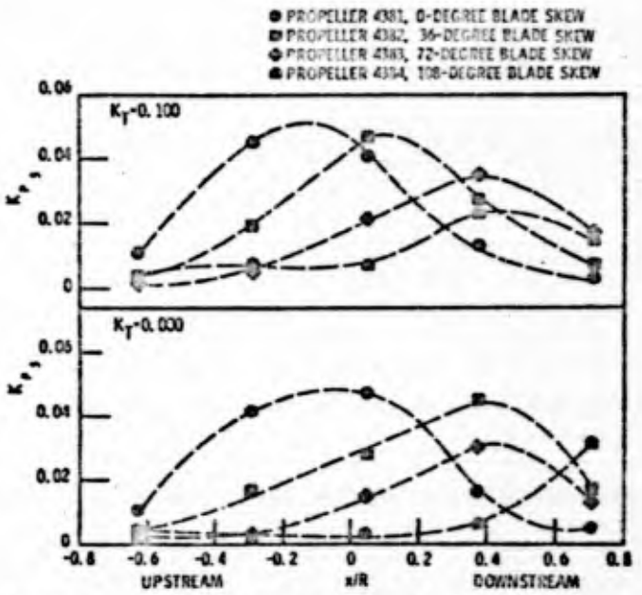

Figure 16 – Measured Blade-Rate Pressure Amplitudes for the Skewed Propeller Series at K_T = 0.100 and K_T = 0.00 for 10-Percent Propeller Radius Tip Clearance

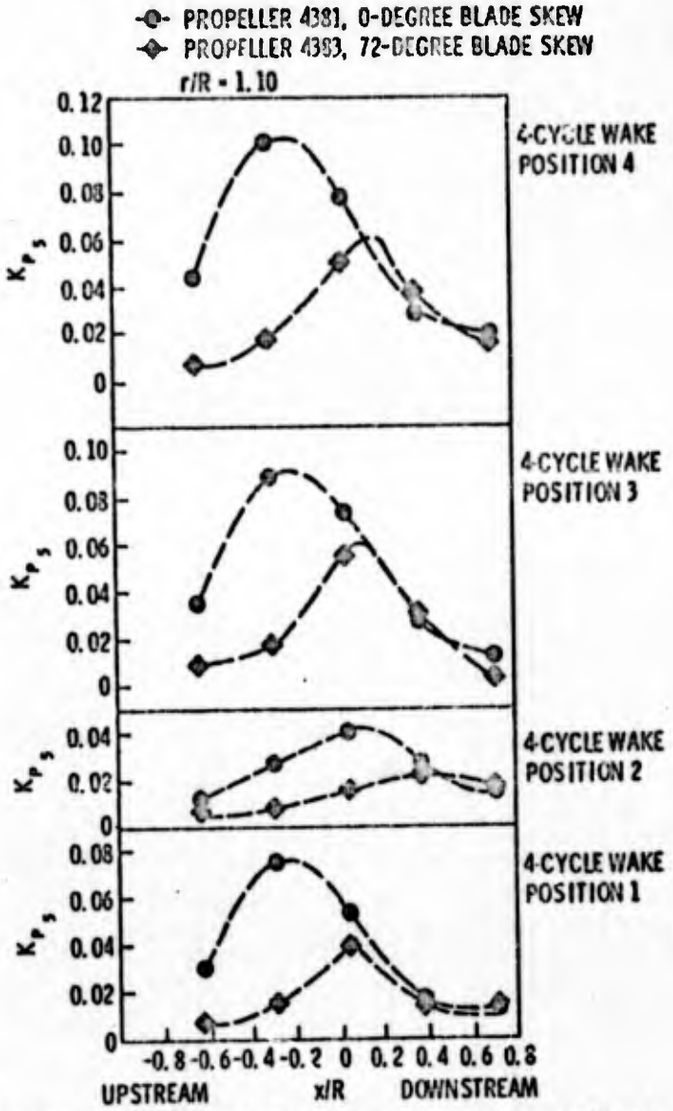

Figure 17 – Measured Blade-Rate Pressure Amplitudes for the 0- and 72-Degree Skewed Propellers at Mean Thrust Coefficient $\overline{K_T} = 0.215$, 10-Percent Propeller Radius Tip Clearance, and Four Distinct Positions of the 4-Cycle Wake Screen

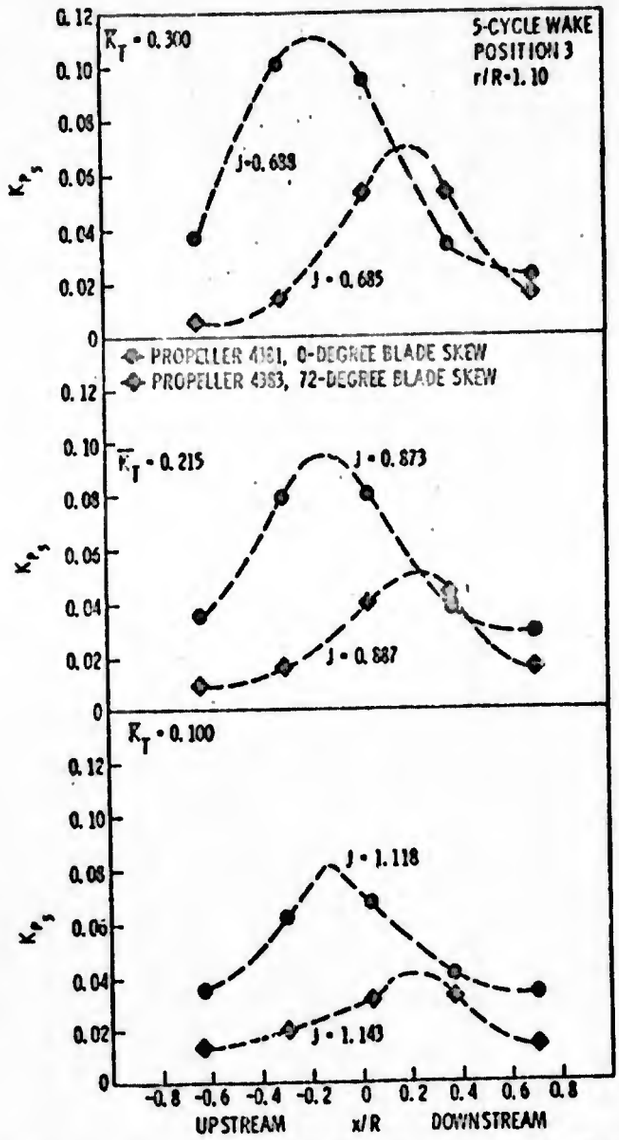

Figure 18 – Measured Blade-Rate Pressure Amplitudes for the 0- and 72-Degree Skewed Propellers at Mean Thrust Coefficient Values $\overline{K_T}$ = 0.300, 0.215, and 0.100 for Position 3 of the 5-Cycle Wake Screen

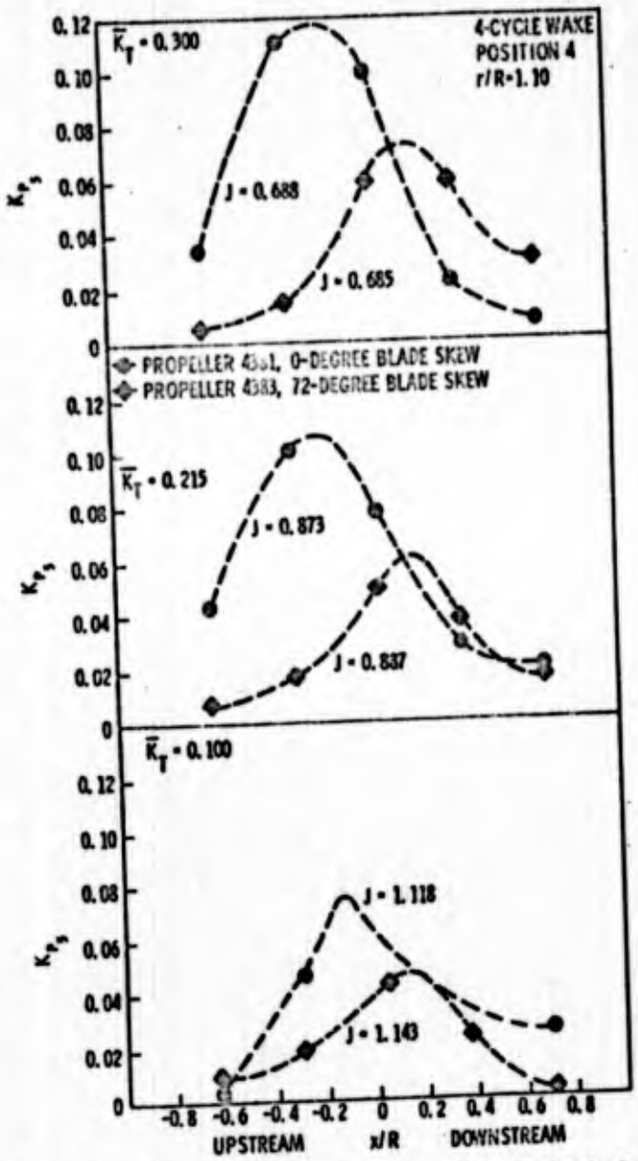

Figure 19 – Measured Blade-Rate Pressure Amplitudes for the 0- and 72-Degree Skewed Propellers at Mean Thrust Coefficient Values $\bar{K}_T$ = 0.300, 0.215, and 0.100 for Position 4 of the 4-Cycle Wake Screen

CONCLUSION

Induced pressures were measured on a flat plate near skewed propellers. There were essentially no harmonics in the pressure signal of comparable size to the blade-rate harmonic. Experimental results from the uniform flow tests at propeller design advance coefficient compared very well in phase and amplitude to the Kerwin blade-rate pressure predictions.

Significant decreases in measured blade-rate pressure amplitude were found to occur for increasing values of blade skew. The peak blade-rate amplitude determined for the nonskewed propeller was reduced by approximately 15, 27, and 51 percent for 36, 72, and 108 degrees of blade skew, respectively, at design advance coefficient in uniform flow and at 10-percent propeller radius tip clearance. Also, because of the natural rake of skewed propellers, the peak amplitude signal was located farther downstream for increasing values of skew. Depending on propeller placement on the ship, these factors could be beneficial in reducing hull vibration created by the induced pressure fluctuations.

A sizeable decay of the blade-rate-induced pressure signal was apparent at a 30-percent propeller radius tip clearance compared to the 10-percent clearance with the propeller operating at the same advance coefficient. It is reasonable to assume that values of induced pressures may be estimated for intermediate clearances by interpolating between these values.

Both uniform flow and nonuniform flow results showed that blade-rate-induced pressures increased with an increase in blade loading. Results of the nonuniform flow tests indicated that a change of the wake region in line with the transducers had essentially the same effect on blade-rate pressure amplitudes as changing the loading by changing the advance coefficient in uniform flow.

REFERENCES

1. Cheng, H. M., "Hydrodynamic Aspect of Propeller Design Based on Lifting-Surface Theory, Part II, Arbitrary Chordwise Load Distribution," David Taylor Model Basin Report 1803 (Jun 1965).

2. Kerwin, J. E. and Leopold, R., "Propeller-Incidence Correction Due to Blade Thickness," Journal of Ship Research, Vol. 7, No. 2 (Oct 1963).

3. Boswell, R. J., "Cavitation and Open-Water Performance of a Series of Skewed Propellers Designed by Lifting-Surface Procedures," NSRDC Report 3339 (in preparation).

4. Boswell, R. J. [redacted] "Design, Cavitation Performance, and Open Water Performance of a Series of Research Skewed Propellers" NAVSHIPRANDCEN 3339, March 1971.

5. Boswell, R. J., "Static Stress Measurements on a Highly Skewed Propeller Blade," NSRDC Report 3217 (Dec 1969).

[redacted]

7. Boswell, R. J. and Miller, M. L., "Unsteady Propeller Loading-Measurement, Correlation with Theory, and Parametric Study," NSRDC Report 2625 (Oct 1968).

8. Tachmindji, A J. and Dickerson, M. C., "The Measurement of Osci'lating Pressures in the Vicinity of Propellers," David Taylor Model Basin Report 1130 (Apr 1957).

9. Kowalski, T. and Breslin, J. P., "Experimental Study of Propeller-Induced Vibratory Pressures on Simple Surfaces and Correlation with Theoretical Predictions," Davidson Laboratory Report 973 (Jul 1963).

10. Denny, S. B., "Comparisons of Experimentally Determined and Theoretically Predicted Pressures in the Vicinity of a Marine Propeller," NSRDC Report 2349 (May 1967).

11. Kerwin, J. E., "Propeller Field Point Velocities," Massachusetts Institute of Technology Report (in preparation).

12. Kerwin, J. E., "A Design Theory for Subcavitating Propellers," SNAME Transactions, Vol. 72 (1964).

13. McCarthy, J. H., "A Method of Wake Production in Water Tunnels," David Taylor Model Basin Report 1785 (Oct 1963).

The Naval Ship Research and Development Center is a U.S. Navy center for laboratory effort directed at achieving improved sea and air vehicles. It was formed in March 1967 by merging the David Taylor Model Basin at Carderock, Maryland and the Marine Engineering Laboratory (now Naval Ship R & D Laboratory) at Annapolis, Maryland. The Mine Defense Laboratory (now Naval Ship R & D Laboratory) Panama City, Florida became part of the Center in November 1967.

Naval Ship Research and Development Center
Washington, D. C. 20034

MAJOR NSRDC ORGANIZATIONAL COMPONENTS

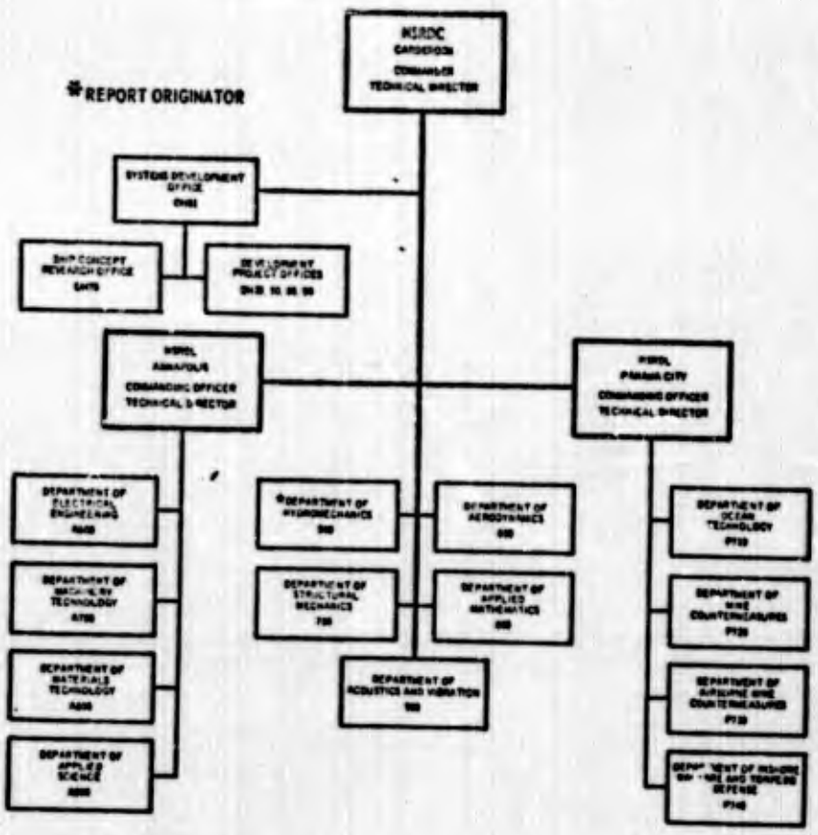

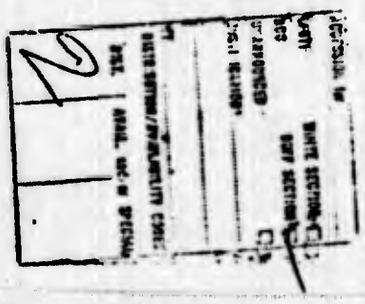

NDW-NSRDC 3960/43 (3-

UNCLASSIFIED
Security Classification

DOCUMENT CONTROL DATA - R & D
(Security classification of title, body of abstract and indexing annotation must be entered when the overall report is classified)

1. ORIGINATING ACTIVITY (Corporate author)
Naval Ship Research and Development Center
Washington, D. C. 20034

2a. REPORT SECURITY CLASSIFICATION
UNCLASSIFIED

2b. GROUP

3. REPORT TITLE
FIELD-POINT PRESSURES IN THE VICINITY OF A SERIES OF SKEWED MARINE PROPELLERS

4. DESCRIPTIVE NOTES (Type of report and inclusive dates)
Final

5. AUTHOR(S) (First name, middle initial, last name)
Stephen S. Teel and Stephen B. Denny

6. REPORT DATE	7a. TOTAL NO. OF PAGES	7b. NO. OF REFS
August 1970	32	13

8a. CONTRACT OR GRANT NO.	9a. ORIGINATOR'S REPORT NUMBER(S)
b. PROJECT NO. S-R009-0101 Problem 526-356	3278
c.	9b. OTHER REPORT NO(S) (Any other numbers that may be assigned this report)
d.	

10. DISTRIBUTION STATEMENT
This document is subject to special export controls and each transmittal to foreign governments or foreign nationals may be made only with prior approval of NSRDC (Code 500).

11. SUPPLEMENTARY NOTES	12. SPONSORING MILITARY ACTIVITY
	NAVSHIPS

13. ABSTRACT

Total fluctuating pressures were measured on a flat plate adjacent to a model propeller operating in the 24-inch water tunnel. The effects of blade skew on propeller-induced field pressures are shown. The amplitude and phase of the blade-rate portions of the measured induced pressures are compared with the Kerwin prediction of propeller field-point pressures for operation in uniform flow at the design advance coefficient and for two propeller tip clearances. Experimental results and theoretical predictions for total field-point pressures were in good agreement for both amplitude and phase.

In addition to the measurements made in uniform flow, induced pressures were also measured for the propellers operating in nonuniform flows generated by 4- and 5-cycle wake screens placed upstream of the propeller. Experimental results of tests in uniform and nonuniform flow at the same mean thrust coefficient showed that increasing blade skew had the effect of reducing propeller-induced pressures and that increasing blade skew displaced the peak amplitude signal farther downstream.

DD FORM 1 NOV 65 1473 (PAGE 1)
S/N 0101-807-6801

UNCLASSIFIED
Security Classification

14 KEY WORDS	LINK A		LINK B		LINK C	
	ROLE	WT	ROLE	WT	ROLE	WT
Propeller-Field Pressures						
Skewed Propellers						
Propeller-Induced Vibration						